

# Using the aerial image measurement technique to speed up mask development for 193nm immersion and polarization lithography

Axel M. Zibold<sup>1</sup>, W. Harnisch, T. Scherübl, N. Rosenkranz, J. Greif  
Carl Zeiss SMS GmbH, Carl Zeiss Promenade 10, D-07745 Jena, Germany

## ABSTRACT

The Aerial Image Measurement System (AIMS<sup>TM</sup>♦) for 193nm lithography emulation is established as a standard for the rapid prediction of wafer printability of critical features, such as dense patterns or contacts, defects or repairs on masks. The benefit of AIMS<sup>TM</sup> is to save expensive image qualification consisting of test wafer exposures followed by wafer SEM measurements. By adjustment of numerical aperture, illumination type and partial coherence to match the stepper or scanner, AIMS<sup>TM</sup> predicts the printability of any 193nm reticle like binary, OPC and PSM. The newly available 193nm 2<sup>nd</sup> generation AIMS<sup>TM</sup> fab systems are able to emulate numerical apertures (NA) up to 0.92 and provide a capability down to 65nm node regardless of the use of an immersion liquid or dry conditions. Rigorous simulation studies have been performed to study the matching of AIMS<sup>TM</sup> and scanner results at NA = 0.92 and to study the extension of the AIMS<sup>TM</sup> technique for immersion lithography emulation of hyper NA up to at least 1.4. Strong polarization effects depending on mask patterns and material as well as imaging effects will occur below the 65nm node. It will be shown that using the polarization capabilities of such a future immersion AIMS<sup>TM</sup> tool will provide a very suitable immersion lithography emulator. Together with low k1 values and polarization effects, 193nm mask design and manufacturing will face increased challenges for design and OPC placement at the 65nm node and below. Aerial image measurements of test masks using AIMS<sup>TM</sup> will then be crucial to speed up mask development. We propose to measure reticles on critical points as defined by simulation or areas of concern for manufacture with the AIMS<sup>TM</sup> system to analyze defect printability and mask manufacturability.

**Keywords:** aerial image measurement, AIMS, photomask, reticle, immersion, numerical aperture, polarization, PSM, OPC, DFM, design for manufacture

## 1. INTRODUCTION

The AIMS<sup>TM</sup> is an optical system for evaluating reticles under the specific stepper or scanner settings of wavelength, numerical aperture (NA), partial coherence of illumination ( $\sigma$ ) and illumination type such as annular, quadrupole or dipole.<sup>1,2,4,7</sup> Both  $\sigma$  and NA are automatically adjustable pupil apertures which cover a wide range of values. They can be adjusted to different exposure tool settings with minimal effort at one and the same system. On a 2<sup>nd</sup> generation AIMS<sup>TM</sup> fab 193 tool standard values are  $0.25 < \sigma < 1$  and  $0.6 < NA < 0.92$ . Whereas typically the scanner is transferring the image with a reduction on the resist of the wafer, the AIMS<sup>TM</sup> images with a total magnification of 150x between mask plane and CCD camera image plane capturing the aerial image in a field of view of about  $60\mu\text{m} \times 60\mu\text{m}$  (standard  $20\mu\text{m} \times 20\mu\text{m}$ ) on the mask.

The 193nm tool is commercially available as a highly automated AIMS<sup>TM</sup> fab 193 and AIMS<sup>TM</sup> fab 193 plus, the latter including mini-environment, mask handling and SMIF capability.<sup>8</sup> The AIMS<sup>TM</sup> tools are state-of-the-art in the photo mask industry for development, defect repair verification, quality control, and defect printability classification of photomasks and reticles. With the emergence of the 65nm node and very low k1 factors the current 1<sup>st</sup> generation

---

<sup>1</sup> zibold@smt.zeiss.com

♦ TM: trademark of Carl Zeiss

Advanced Microlithography Technologies conference in Beijing, 2004, Proceedings of SPIE 5645-30

AIMS™ fab 193 tool has undergone a series of system improvements to make it suitable for the highly automated and efficiency sensitive production environment. Such new 2<sup>nd</sup> generation AIMS™ fab 193 plus has significantly higher throughput, improved stability, new illumination energy monitoring for better CD repeatability and a new beam homogenizer for improved field homogeneity in addition to other system improvements.<sup>4</sup> The 2<sup>nd</sup> generation 193nm system is very suitable to cover the production requirements of  $NA < 1$  for both dry and immersion lithography. For the latter utilizing an extended depth-of-focus software. An upcoming option to upgrade linear polarization in illumination will also provide an excellent opportunity to do early R&D work in order to investigate polarization effects arising from the mask itself.

The 2<sup>nd</sup> generation 193 system including the polarization and extended depth-of-focus system will be available as AIMS™ fab 193i. Figure 1 shows a picture of the 2<sup>nd</sup> generation AIMS™ fab 193 plus.



Fig. 1: Picture of an AIMS™ fab 193 plus, an automated AIMS™ system including mask handling.

Figure 2 shows the field of view of dense 1:1 lines and spaces of 300nm feature size on an attenuated PSM reticle. The field of view is  $4.5\mu\text{m} \times 4.5\mu\text{m}$  at the wafer level taking the 1:4 reduction of the scanner into account. A through focus series was taken with 5 images. The settings have been  $NA = 0.9$  and circular  $\sigma = 0.75$ . The aerial image (upper left plot) represents the focal plane commonly called best focus. The image is normalized by a reference image taken on a clear area of the reticle and applying the exact same settings. The intensity profile plot (upper right plot) allows the evaluation of maximum peak intensities of the bright features and comparison to one another for all planes measured in the through focus series. In case of a defect a change of an individual peak intensity can be found and printability determined by comparison of defect intensity and neighbouring feature intensity.

The cursor in the profile plot selects one feature for further evaluation. The linewidth versus threshold plot (lower left plot) provides the opportunity to analyze the predicted linewidth for the different focal layers for a selected threshold value. The “Pivot”-point, where the predicted linewidth does not depend on the focal position can be clearly seen. In our case a threshold of 0.109 is selected and the predicted linewidth prints to 80nm at best focus on the wafer level. The linewidth analysis of the threshold model is another way to determine printability of features or defects by comparison of different linewidth values of neighbouring features of the same structure and size.

Based on the through-focus measurement, further mask structure or feature analysis can be performed either looking at the Bossung plot, i.e. linewidth versus defocus, or the exposure-defocus plot. An example the exposure-defocus window (lower right plot) is displayed to extract information about the defocus tolerance. Selecting 8% exposure tolerance for a target CD value of 80nm on the wafer and  $\pm 10\%$  linewidth tolerance (lower right plot), a defocus tolerance of  $0.19\mu\text{m}$  is found. Thus the exposure-defocus window analysis is a generalization which allows us to consider simultaneously the impact of focus and exposure dose tolerance on the target linewidth value of a mask structure. Taken at several field points it allows the extraction of the common process window from the various overlapping areas and predicts printability in general.

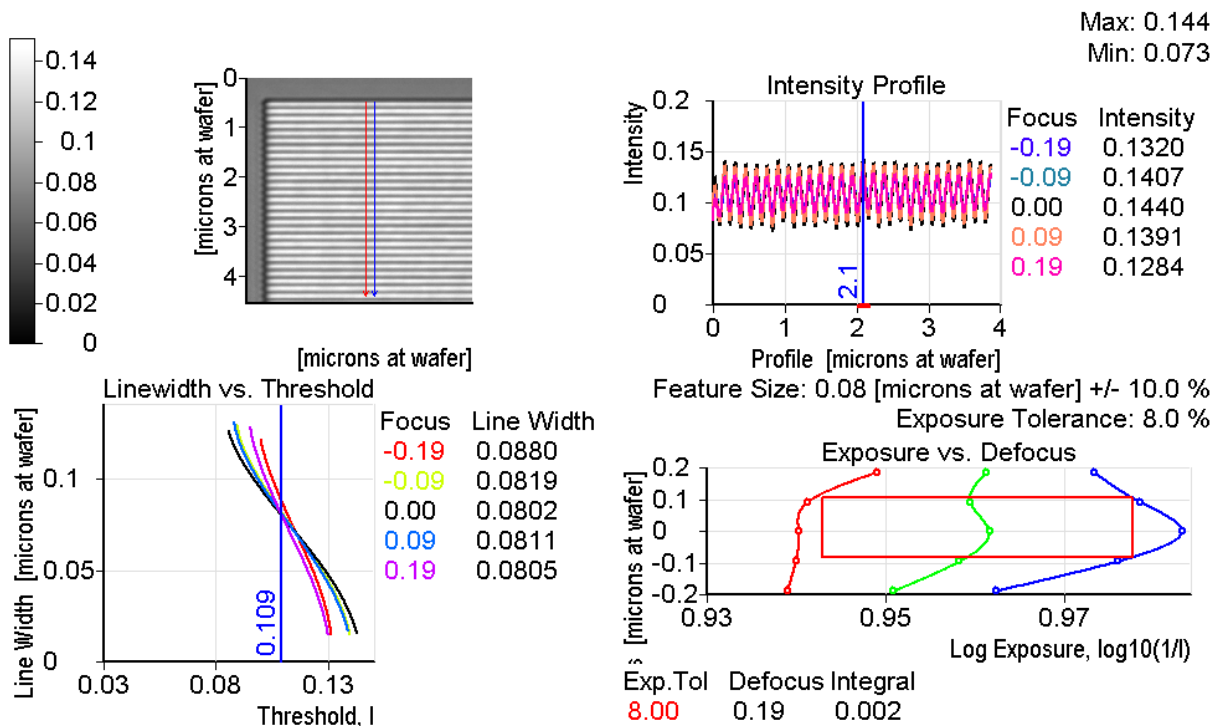


Fig. 2: Lines and spaces measurement of 300 nm at PSM mask features and data evaluation of peak intensities, linewidth behaviour and exposure defocus window utilizing the through-focus measurement capability of the 193nm AIMS™

## 2. COMPARISON IMMERSION EXPOSURE TOOL AND AIMS

Ongoing discussions show expectations towards 193nm immersion lithography in order to realise a 32nm node or even smaller.<sup>5</sup> Scanner lens designs are expected to achieve numerical apertures of 1.2 and higher.<sup>6</sup> It is the so-called hyper NA range with  $NA > 1$ .

Figure 3 shows a schematic comparison between the scanner or stepper and an AIMS™ tool. In the dry system with air between the imaging optics and the wafer the maximum numerical aperture at the wafer side is  $NA < 1$ . For example having a numerical aperture of  $NA = 0.92$  on the wafer side of the scanner and a reduction optics 1:4, the numerical aperture at the imaging side of the mask is  $NA_{im} = 0.92 / 4 = 0.23$ . The same  $NA_{im} = 0.23$  on the imaging side of the mask is realized in the AIMS™ tool. On the AIMS™ tool for adjustment of the equivalent variable NA values in the range  $0.6 < NA < 0.92$  pinholes different in size can be automatically moved into a conjugated pupil plane close to the CCD camera plane.

By adding an immersion liquid between the imaging optics and the resist on the wafer, an effect of extended depth-of-focus (EDOF) can be achieved.<sup>3</sup> In the case where the size of the imaging optics is not enlarged and the numerical aperture on the imaging side of the mask is still  $NA_{im} = 0.23$ , there is no gain in resolution enhancement or in printability to smaller feature size. This is due to the fact that the maximum capture angle between 0 and 1<sup>st</sup> order diffraction orders from an object on the mask is not increased.

Thus for the AIMS™ fab 193 2<sup>nd</sup> generation tool with  $NA < 1$  we have to take into account the effect of EDOF only. This will be described in the section 3.

In the case where an immersion liquid is used and the size of the imaging optics is sufficiently enlarged, to allow larger capture angles between 0 and 1<sup>st</sup> order diffraction, capturing of 1<sup>st</sup> orders from smaller objects on the mask become possible. Such a hyper NA tool can be used to print feature sizes below the 65nm node. If we just assume a NA = 1.6 on the wafer and 1:4 reduction system then this results in a numerical aperture at imaging side of the mask  $NA_{im} = 1.6 / 4 = 0.4$ . As a consequence a hyper NA AIMS<sup>TM</sup> tool requires a new beam line with bigger pupil diameters for larger capture angles to be designed in addition to other major tool improvements. There is also no need to have an immersion liquid on such an AIMS<sup>TM</sup> system.

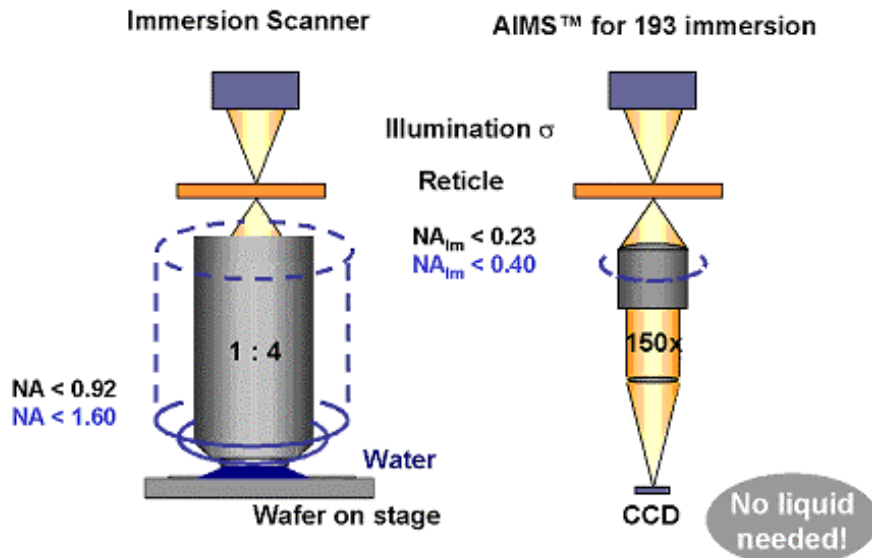


Fig. 3: Comparison between immersion scanner or stepper and AIMS<sup>TM</sup>

### 3. EDOF

With smaller exposure wavelengths and larger NA the printing of smaller feature sizes becomes especially critical due to a smaller useable depth-of-focus. With smaller linewidth a general shrinking of the size of the exposure-defocus window can be observed. Based on the through-focus aerial image measurement it is possible to display the exposure-focus window in the AIMS<sup>TM</sup> software showing the maximum allowable focus variation at a given specified exposure tolerance. For dry lithography emulation (1:4) the allowable focus variation can either be displayed for focal coordinates at the mask level ( $z_m$ ) or for focal coordinates at the wafer level ( $z_w = z_m/16$ ). By switching to immersion (wet) lithography emulation the variation for focal coordinates on mask level does not change for either the wet or dry condition. However for the transition to focal coordinates on wafer level we have to consider for wet conditions the refractive index of the immersion liquid between the imaging optics and the resist on the wafer. The well-know Rayleigh criterion has to be modified as described by C. Mack et al.<sup>3</sup> Therefore for calculations at the wafer level the AIMS<sup>TM</sup> software is now taking the advanced focus calculation into account for all plots related to the through-focus behaviour such as linewidth or contrast versus defocus, process window, etc. An example, for the process window we find that the allowable focus variation at a fixed exposure tolerance becomes enlarged with a larger refractive index of the immersion liquid.

In this work we have investigated the results of dense 1:1 lines and spaces of 300nm feature size on an attenuated PSM reticle. The settings are described in chapter 1. For a target CD value of 80nm on the wafer and +/-10% linewidth tolerance we find at a 10% exposure tolerance an increase of the defocus tolerance from 0.14 $\mu$ m to 0.23 $\mu$ m by using a water immersion liquid with refractive index  $n = 1.44$  instead of air with  $n = 1$ . A comparison of the size of the process window with and without immersion liquid is shown in figure 4 (left plot). The right plot in figure 4 shows the increase of the process latitude with larger refractive index.

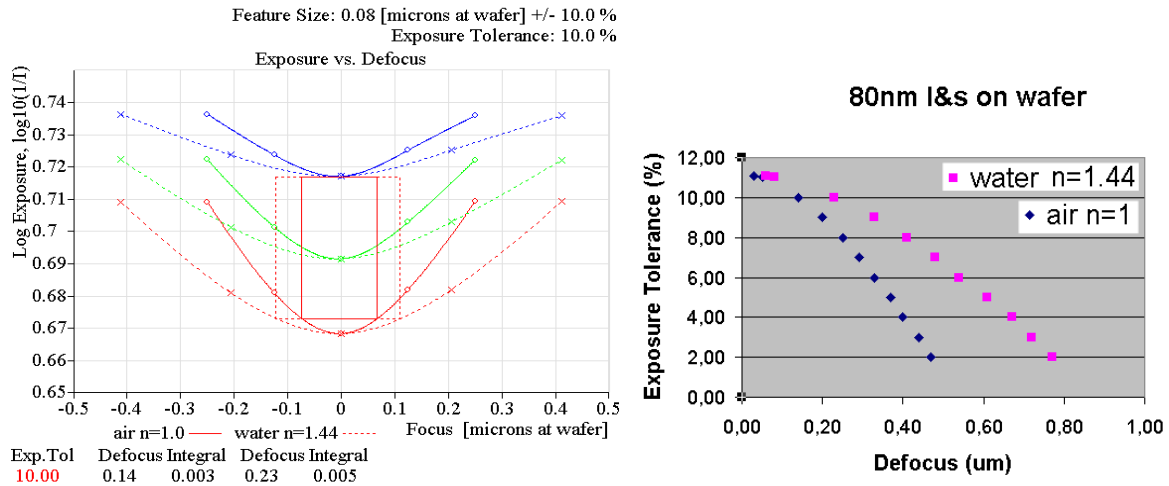


Fig. 4: Exposure tolerance versus defocus for dry condition and water immersion at fixed numerical aperture

## 4. DISCUSSION OF POLARISATION EFFECTS FOR AIMS

### 4.1 Polarization effects from imaging

It is generally known that with an increase of the numerical aperture on scanners or steppers to very high NA values polarization effects will occur resulting in a loss of contrast for the p-type polarized light contribution.<sup>3</sup> Considering the 1:4 reduction of the scanner or stepper and the 150x magnification on the AIMS™, the scanner is having large angles of incident light between resist and imaging optics (lens space), whereas the AIMS™ has smaller angles of incident light on the CCD camera plane which is the equivalent image plane to capture the latent resist image. Therefore the contrast loss at very large angles is expected to not be seen in the AIMS™ and has to be additionally emulated. However, since the aerial images from the AIMS™ are compared to the printing features in resist -obtained by test wafer exposures followed by SEM measurements- the appropriate comparison is always the aerial image of the AIMS™ to the resist image of the scanner.

Firstly the question arises, how do such polarization effects occur at the limit of NA close to but less than 1? Considering a large numerical aperture or large angles of incident waves in the lens space, the angles of the propagating waves into the resist are significantly smaller due to the larger refractive index of the resist, (e.g.  $n_R=1.7$ ) compared to  $n=1$  in air, as can be seen by Snell's law. Therefore we can expect in a printing process with high numerical apertures but still  $NA < 1$  a rather small contribution of polarization effects from imaging. This situation remains the same if an immersion liquid is added into the lens space. For  $NA < 1$  looking at the propagation of the light from mask object to resist, we find that the angle of the interfering waves in the resist are independent of the medium filled into the lens/ resist space based on Snell's Law.<sup>3</sup> Important for printing is the angle of the interfering waves in the resist which always have the numerical aperture  $\ll 1$ . Therefore for  $NA < 1$  independent of an immersion liquid or air in the lens space of an exposure tool, polarization effects in the resist are expected to be small compared to hyper NA and only an increased depth-of-focus should be considered.

To investigate these polarization issues more in detail we have performed simulations using a rigorous coupled waves analysis simulation realized within an in-house simulation software of Carl Zeiss. This simulation takes the interaction of the electromagnetic field vectors and the three-dimensional structure of the mask features into account. The reflection and transmission behaviour on the interface between resist and medium of the lens space has also to be considered. Simulations are performed for  $NA = 0.92$  and  $NA = 1.4$  for both the scanner image latent in the resist and the aerial image of an AIMS™.

Figure 5 (upper plots) compares intensity profile plots of aerial image results of AIMS™ with resist images from a scanner for 500nm binary line and space mask features chrome on quartz. A very good match can be found however, the AIMS™ has slightly higher peak intensities compared to the scanner results. The lower plots show the relative difference of the linewidth between scanner and AIMS™ results versus threshold using a straight forward threshold model. We can see that for a large range of thresholds the CD results are matching with  $\ll 2\%$ . The results are also displayed for best focus and 2 different out-of-focus layers. The same results have been seen for different focal layers. Similar results on AIMS™ and scanner matching for NA = 0.92 have also been found for 400nm line and space simulations.

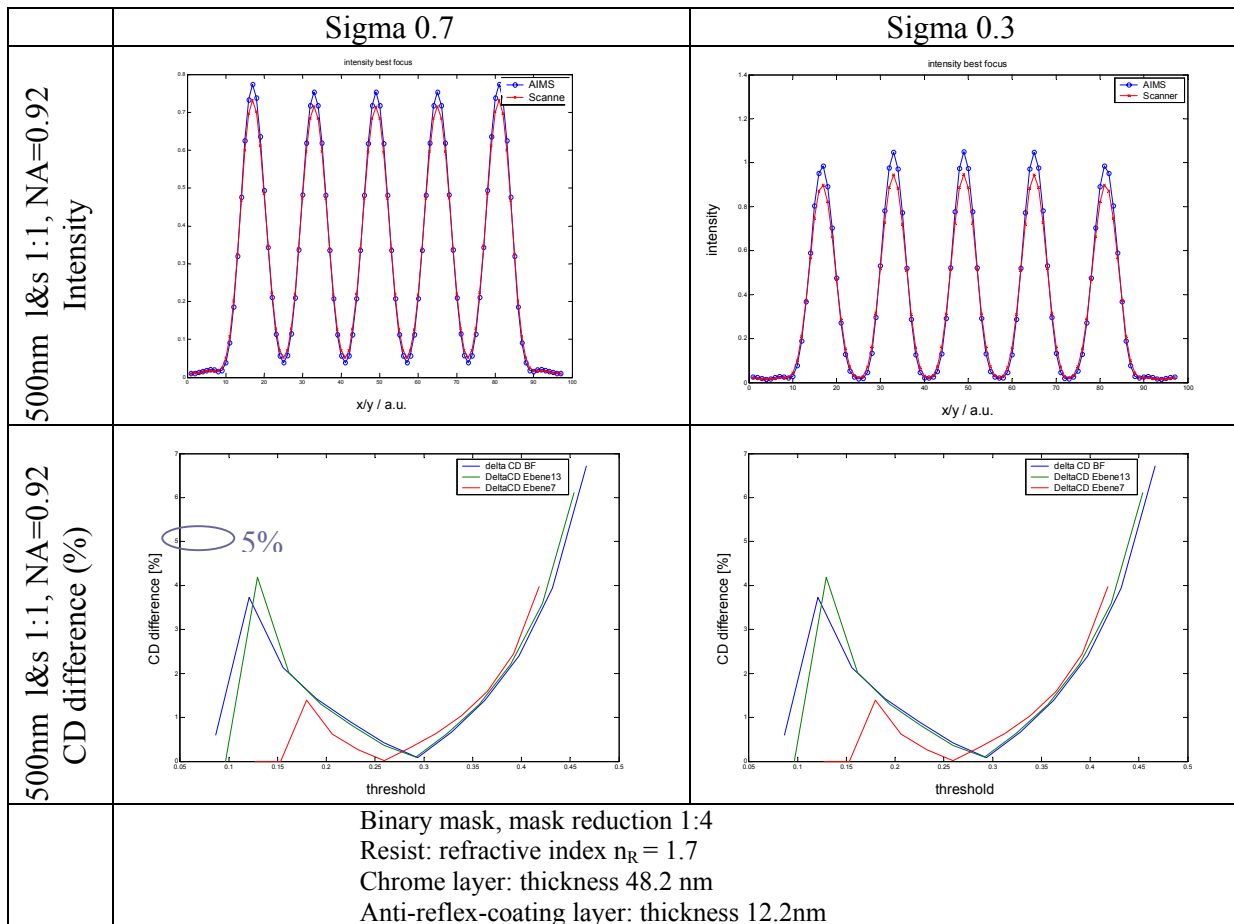


Fig. 5: Comparison of the aerial image results on AIMS™ and the resist image results of a scanner for 500nm binary mask features

Thus from the comparison we can find a very good matching of AIMS™ and scanner results for such a NA < 1 system. The deviations seen for maximum peak intensities indicate that criteria for printability results on AIMS™ have to be based on CD criteria at intermediate thresholds instead of transmission loss criteria as is commonly performed at larger nodes.

It can also be concluded that the 2<sup>nd</sup> generation AIMS™ fab 193 is very suitable for scanner/stepper emulation for both immersion and dry systems in the area of numerical apertures up to 0.92 for the 65nm node.

In a further step we have investigated polarization effects for hyper NA systems. As discussed in chapter 2 these exposure tools will have larger lens diameters and therefore we will also find increased angles of the incident waves into the resist. Polarization effects from imaging are expected when NA  $\gg 1$ .

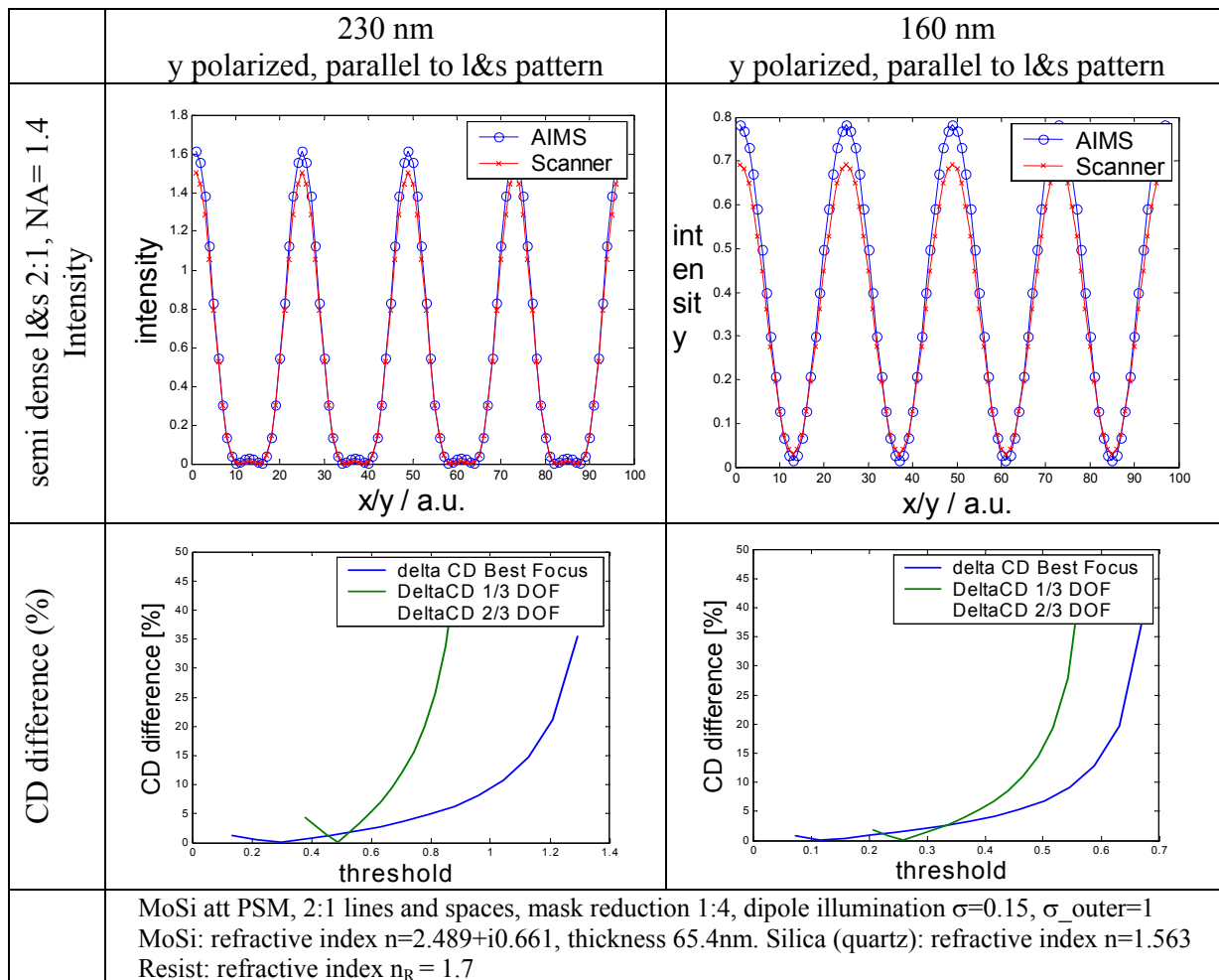


Fig. 6: Comparison of the aerial image results on AIMS™ and the resist image results of the scanner for 230 nm and 160 nm MoSi att PSM mask features

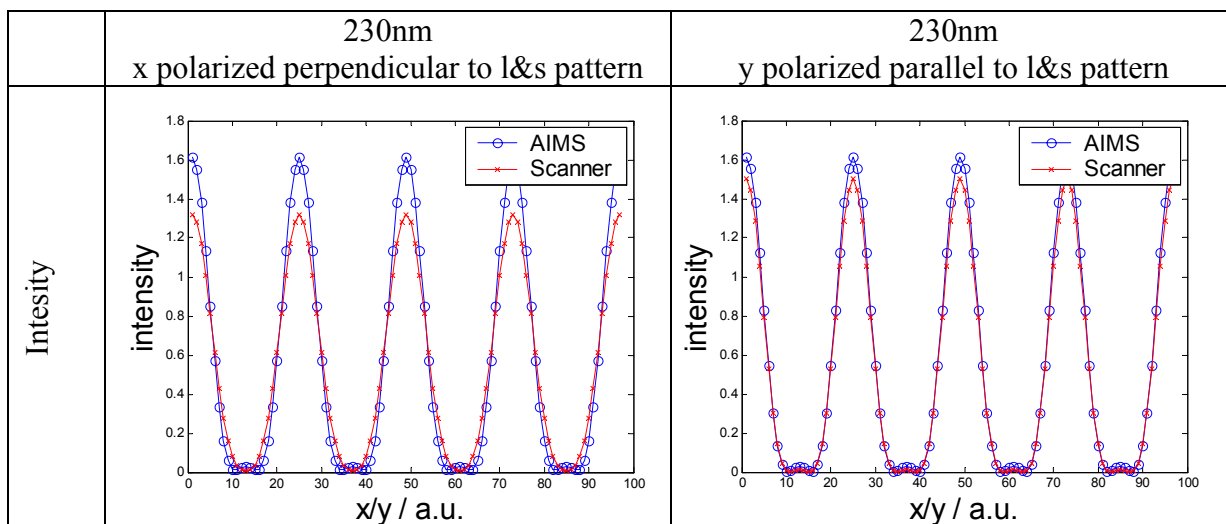


Fig. 7: Comparison of the aerial image results on AIMS and the resist image results of the scanner for 230 nm MoSi att PSM mask features for linear polarization parallel and perpendicular to the lines and space pattern.

Figure 6 compares intensity profile plots of aerial image results using AIMS™ and of resist images from a scanner for 230nm and 160nm attenuated MoSi PSM mask features. The illumination used is a dipole setting and linearly polarized parallel to the structure which approximates a s-type polarization. A good match can be found. However with smaller feature sizes the AIMS™ results have increasingly higher relative peak intensities compared to the scanner results. The lower plots of figure 6 show the relative difference of the linewidth between scanner and AIMS™ results versus threshold using a straight forward threshold model. The results are displayed for best focus and one out-of-focus layer. We can find for larger threshold  $> 0.4$  that the deviation of CD results from AIMS™ and scanners are increasing strongly. The deviations become even larger for the out-of-focus results.

In figure 7 the simulations were performed for 230nm line and space features including x (parallel to the lines & spaces pattern) and y polarization (perpendicular to the lines & spaces pattern) in illumination. The plots compare intensity profiles of aerial image results on AIMS™ and of resist images from a scanner. From the relative difference of the maximum peak intensities it can be seen that AIMS™ and scanner are matching better for polarized illumination parallel to the lines & spaces pattern. An unpolarized illumination in this case will result in an average of the x and y polarized profile plot.

Optimized polarization in illumination will clearly reduce polarization effects in exposure tools and also provide closer correspondence with the AIMS™. Linear polarization in the illumination combined with an appropriate off-axis pattern shape will help to reduce the contrast loss in the lithographic process. To realize a hyper NA scanner emulation AIMS™ tool there is an ongoing project at Carl Zeiss for designing a new beam path and totally new platform. This future hyper NA AIMS™ tools will have additional emulation capability in order to emulate the polarization effects with increasing hyper NA and unpolarized illumination to provide a close match to any given exposure tool.

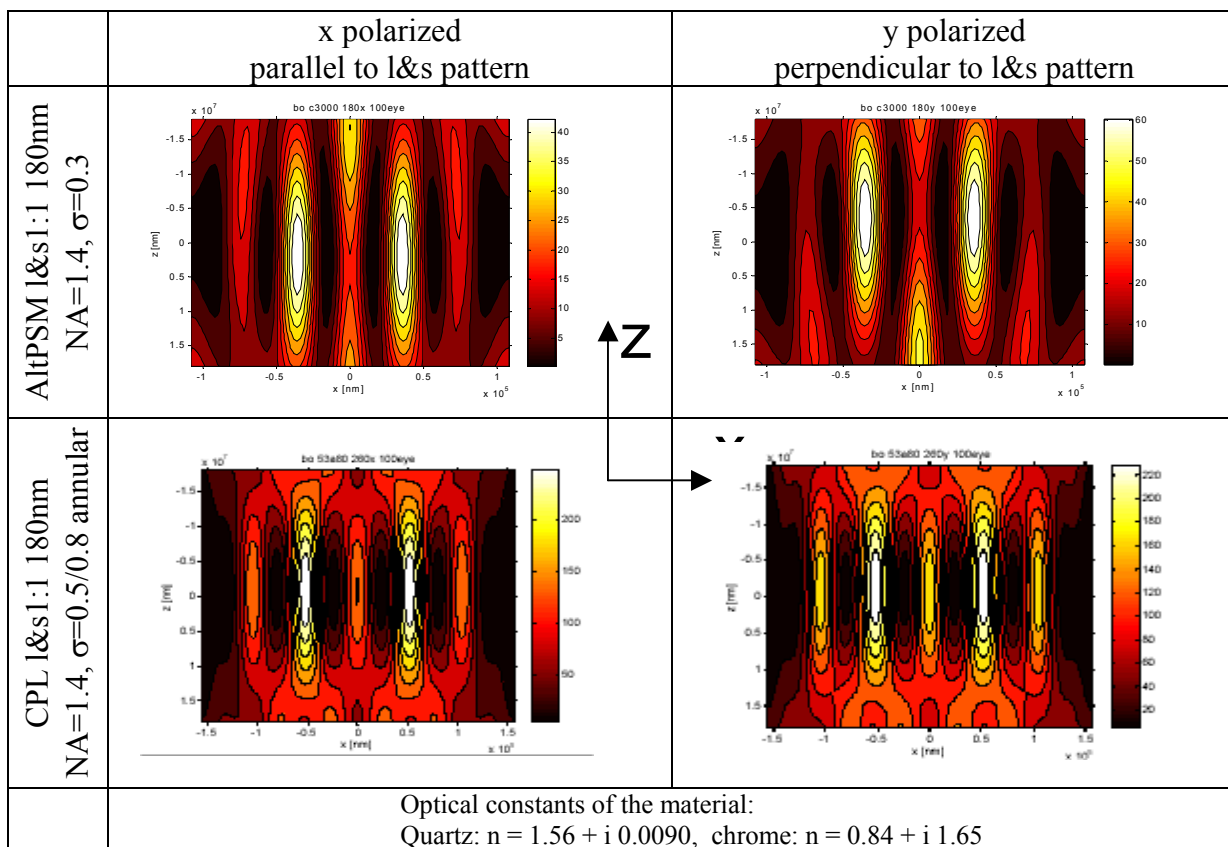


Fig. 8: Comparison of polarized focal aerial images for 2 different mask materials

## 4.2 Polarization effects from mask

A further topic to be addressed is the polarization effects that arise from mask material itself. In general one can say that a pure phase shift mask introduces the smallest polarization effect. The choice of the metal in the absorbing layer influences how pronounced any polarization effect occurs.

Rigorous simulation as described above has been performed for 2 different types of masks: alt PSM and CPL. Figure 8 shows a comparison of focal aerial image results of the best focus planes for x and y polarization. For the alt PSM we can see a strong focal shift and a difference in contrast for the 2 different polarization directions.

To allow early mask R&D investigations of material dependent polarization effects the 2<sup>nd</sup> generation AIMS fab 193 will be equipped in future with a linear polarization capability in the illumination. Polarization effects from mask can then be investigated by measuring transmission loss and difference in contrast for unpolarized and polarized illumination conditions. Deviations in results will allow conclusions on effects of polarization from structures and different mask materials to be drawn. First measurement results are expected to be published soon. In addition it will also allow the emulation of dry scanners with polarized illumination capability for  $NA < 1$ .

## 5. NEW APPLICATION FOR AIMS

As mentioned in the introduction, the AIMS<sup>TM</sup> tools are state-of-the-art in the photo mask industry for development, defect repair verification, quality control, and defect printability classification of photomasks and reticles. Especially the determination of defect repair success in mask shops is a very strong application, because the mask shop can easily adopt the system to the various scanner or stepper settings used in different wafer fabs and does not need to do printability tests on exposure tools. It is common sense that together with polarization effects and low  $k_1$  values at the 65nm node and below, 193nm mask design and manufacture will face increased challenges for design and OPC placement. Aerial image measurement of test masks or full field masks using AIMS<sup>TM</sup> will then be crucial in speeding up the mask development cycle. We propose to measure reticle simulation critical points or areas of concern for manufacturability with the AIMS<sup>TM</sup> system and analyze them for their printability and manufacturability. Figure 9 (left plot) shows a layout image with a marker of a critical point. By using coordinate information on the AIMS<sup>TM</sup> system such a region can be re-visited and the aerial image under the exposure tool conditions acquired. A matching of layout image with marker and aerial image allows us to find the critical point and to extract required information such as linewidth, etc. Such printing result can be fed back to the design and OPC functions for improvement. With the recent AIMS<sup>TM</sup> tool and software improvements, measurements of many such points in an automated way are conceivable.

Such measurements will allow to understand at a very early phase in mask manufacturing the validity of mask design and OPC based on the wafer printability of reticles however independent of the resist and lithographic process infrastructure itself since the AIMS<sup>TM</sup> allows to distinguish between reticle, exposure tool and resist effects avoiding costly and time consuming test exposures.

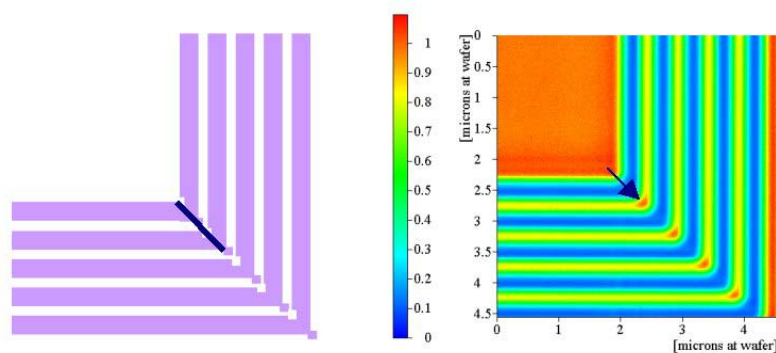


Fig. 9: Comparison of layout image and aerial image. The layout shows a marker to indicate the linewidth for CD evaluation in the aerial image after overly. The corresponding clear space on the aerial image is indicated by the arrow.

## SUMMARY

The 2nd generation AIMS™ fab 193 for stepper or scanner emulation up to NA of 0.92 has been introduced to the market. This system fulfils the requirements of the 65nm node. An extended depth-of-focus software will allow us to emulate the effects of the immersion liquid. From rigorous simulations we have shown that polarization effects from imaging can be neglected and aerial image emulation of the AIMS™ will match well with the resist image from a scanner.

A linear polarized illumination capability is under development to become available with an upgrade of the illumination unit. This will be beneficial and allow early mask R&D work with regard to polarization effects.

To emulate scanners or steppers with hyper NA > 1 a new beam line in addition to major tool improvements has to be designed. From rigorous simulations we can see that polarization effects from imaging and reticle have to be taken into account.

Since the polarization effects depend strongly on the wavelength used for the lithographic process and the mask material, it is very important to optically measure printability using an AIMS™ tool with the same exposure wavelength and stepper/ scanner equivalent NA and  $\sigma$  settings, in order to interpret the imaging properties of the mask relevant for wafer production correctly.

With increasingly complex masks the AIMS™ can be used as a powerful tool not only for defect analysis but also for design or OPC verification to avoid costly and time consuming image qualification through exposure tools. In this way the industry will be able to shorten the design to manufacture time. Future work will address this topic.

## ACKNOWLEDGEMENT

The authors would like to thank Oliver Kienzle, Mark Joyner, Matthias Waechter, Arne Seyfarth, Hans von Doornmalen, Rainer Schmied, and Peter Schaeffer for their discussions related to the topics.

## REFERENCES

1. R.A. Budd, D.B. Dove, J.L. Staples, R.M. Martino, R.A. Furguson, J.T. Weed. Development and application of a new tool for lithographic mask evaluation, the stepper equivalent Aerial Image Measurement System, AIMS. IBM J. Res. Develop. Vol 41 No.1,2 January/ March, 1997.
2. R.A. Budd, J. Staples and D. B. Dove. A New Tool for Phase Shift Mask Evaluation, the Stepper Equivalent Aerial Image Measurement System AIMS. Proceedings of SPIE Vol. 2087, 1993.
3. C.A. Mack and J.D. Byers. Exploring the Capabilities of Immersion Lithography Through Simulation. Proceedings of SPIE Vol. 5377, 2004.
4. A.M. Zibold, T. Scherübl, A. Menck, R. Brunner, J. Greif. Aerial Image Measurement Technique for Today's and Future 193nm Lithography Mask Requirements. Proceedings of 20th EMC Conference, 2004.
5. F.M. Schellenberg, Resolution Enhancement Technology: The Past, the Present, and Extensions for the Future. Proceedings of SPIE Vol. 5377, 2004.
6. B. Streefkerk, J. Baselmans, W. Gehoel-van Ansem, J. Mulkens, C. Hoogendam, M. Hoogendorp, D. Flagello, H. Sewell, P Graeupner. Extending optical lithography with immersion. Proceedings of SPIE Vol. 5377, 2004.
7. A.M. Zibold, R. Schmid, B. Stegemann, T. Scheruebl, W. Harnisch, Y. Kobiyama. Aerial image measurement technique for Automated Reticle Defect Disposition (ARDD) in wafer fabs. Proceedings of SPIE Vol. 5446-117, 2004.
8. A.M. Zibold, R. Schmid, K. Böhm, R. Birkner. Aerial Image Measuring System at 193nm – a tool to tool comparison and global CD mapping. Proceedings of SPIE Vol. 5567-118, 2004.